

Liquid-Liquid Flow Porometry

Dr. Akshaya Jena and Dr. Krishna Gupta
Porous Materials, Inc
Ithaca, NY, USA

Contents

1. Introduction
2. Principle of Liquid-Liquid Flow Porometry
 - 2.1 Relation between Pore Diameter and Pressure
 - 2.2 Measurable Properties
3. The Technique
4. Application
 - 4.1 Wetting Liquids
 - 4.2 Interfacial Tension between Silwick and Isopropyl Alcohol;
 - 4.3 Pore Structure of Membrane
 - 4.3.1 Investigation using LLP
 - 4.3.2 Investigation using CFP
 - 4.4 Pore Structure of Stretched Polymeric Membrane
5. Strengths and Limitations of LLP and CFP
6. LLP with Accurate Bubble Point Detection Capability
7. Summary and Conclusion
8. References

1. Introduction

Many techniques are available for evaluation of pore structure [1]. For characterization of filtration media, Capillary Flow Porometry is widely used because the pore structure characteristics relevant for filtration such as pore throat diameter, largest pore throat diameter, and pore distribution are measurable by this technique [2]. In this technique, the pores of the sample are filled with a wetting liquid and the differential pressure of an inert gas is increased on the sample. Gas under pressure removes the wetting liquid from pores and flows through the empty pores (Figure 1a). The pressure needed to empty a pore is inversely proportional to pore diameter and smaller pores are emptied with increasing pressure. Flow rate of the gas is

measured through the wet sample as a function of differential gas pressure. The flow rate of the same gas is also measured as a function of differential pressure through the dry sample. The measured flow rates and differential pressures are used to compute the relevant pore structure characteristics. When the pores of the filtration media are in the nanometer range, the required test pressure becomes very high. The high pressure often damages the sample and distorts the pore structure. The novel technique, Liquid-Liquid Flow Porometry is capable of measuring the pore structure characteristics relevant for filtration in the nanometer range using a considerably lower test pressure.

2. Principle of Liquid-Liquid Flow Porometry

Liquids capable of spontaneously filling the pores of a sample are known as wetting liquids. For liquid-Liquid Flow Porometry, the pores of the sample are filled with a wetting liquid. A second wetting liquid having surface tension higher than the first wetting liquid and immiscible with the first wetting liquid is selected. Pressure of the second wetting liquid is increased on the sample. The second wetting liquid removes the first wetting liquid from pores and flows through pores (Figure 1b). The flow rate of the second wetting liquid through the sample is measured as a function of differential pressure in the absence of the first wetting liquid in pores (dry curve) and in the presence of the first wetting liquid in the pores (wet curve). The pore structure characteristics are computed from these measured dry and wet curves.

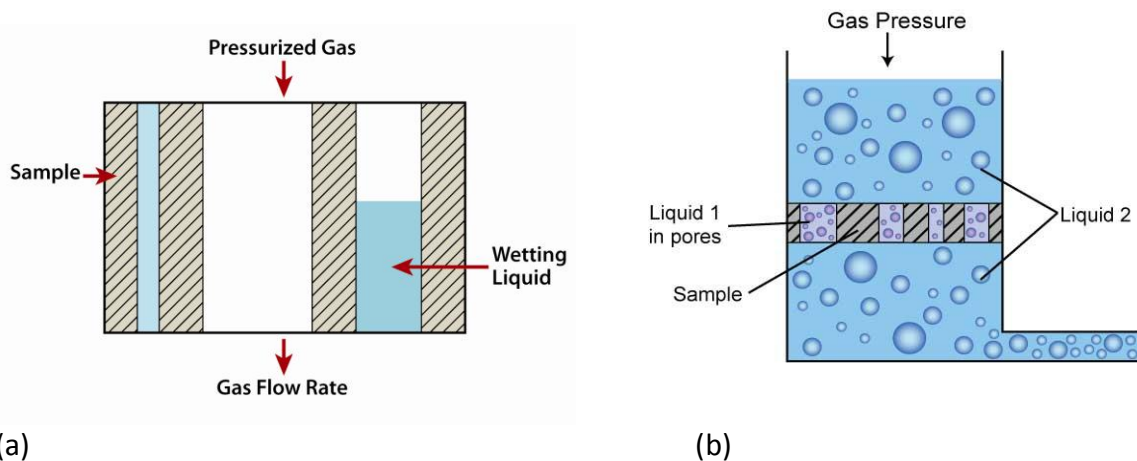


Figure 1. (a) Displacement of a wetting liquid from pores by a pressurized gas
(b) Displacement of one wetting liquid from pores by another pressurized wetting liquid

2.1 Relation between Pore Diameter and Pressure

Consider displacement of wetting liquid-1 from a pore by wetting liquid-2 (Figure 2). Equating the work done by liquid-2 to the increase in surface free energy,

$$p \, dV = dS (\gamma_{s/L2} - \gamma_{s/L1}) \quad (1)$$

where p is differential pressure on the pore, dV is the small volume element of the wetting liquid displaced in the pore, dS is the change in the surface area due to displacement of the volume element, $\gamma_{s/L2}$ is the surface free energy of solid/liquid-2 interface and $\gamma_{s/L1}$ is the surface free energy of solid/liquid-1 interface.

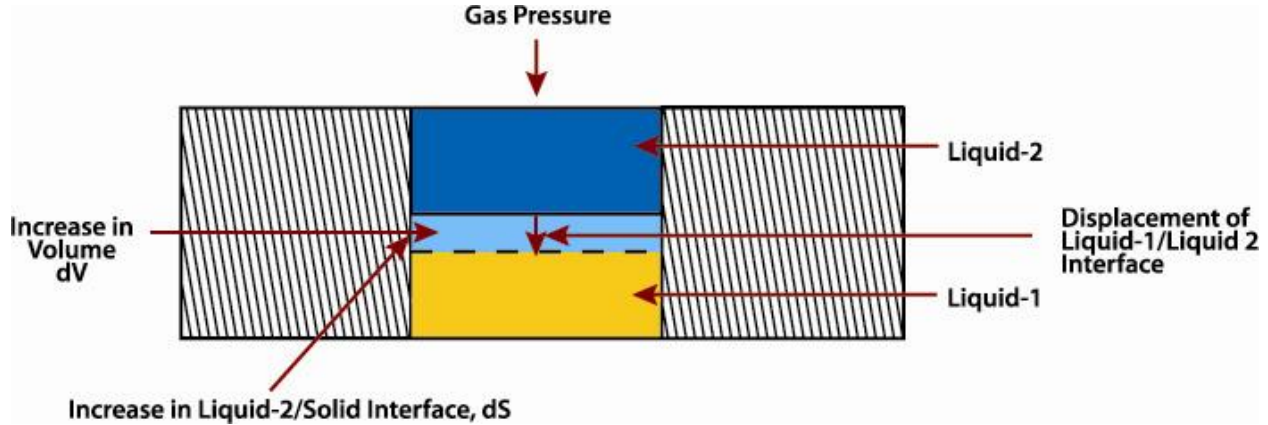


Figure 2. Displacement of wetting liquid-1 in the pore by wetting liquid-2

Pore diameter at the pore cross-section of interest is defined as the diameter of a cylindrical opening whose (dS/dV) is the same as that of the pore at its cross-section of interest. Hence, $(dS/dV) = 4/D$ and Equation 1 reduces to the following.

$$p = 4(\gamma_{s/L2} - \gamma_{s/L1}) / D \quad (2)$$

Making use of the equilibrium between surface tensions depicted in Figure 3, Equation 2 can be further reduced to the following.

$$p = 4 \gamma_{L1/L2} \cos \theta / D \quad (3)$$

where $\gamma_{L1/L2}$ is the interfacial tension and θ is the contact angle. Normally, the surface tensions of the two wetting liquids are small and the interfacial tension, $\gamma_{L1/L2}$ is also very small. Consequently, the contact angle may be assumed to be close to zero and $\cos \theta = 1$. Hence,

$$p = 4 \gamma_{L1/L2} / D \quad (4)$$

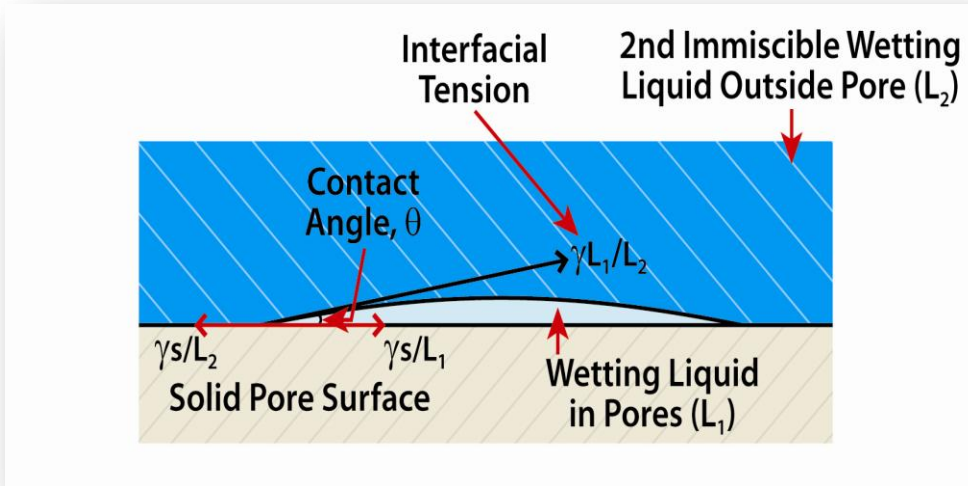


Figure 3. Equilibrium between surface tensions

2.2 Measurable Properties

Differential pressure starts flow through a pore only when the pore is completely emptied. Differential pressure sufficient to displace liquid from the pore throat is capable of removing the liquid completely from the pore. Therefore, differential pressure enabling flow through a pore yields the diameter of the through pore.

The largest through pore throat diameter (Bubble point pore diameter) is computed from differential pressure needed to initiate flow through the wet sample. The mean flow pore diameter is computed from mean flow pressure. The mean flow pressure is the pressure at which the wet flow is the same as half of the dry flow. Pore distribution is computed from dry and wet flows using the following equation.

$$f = - d[(F_w/F_d)_p \times 100] / dD \quad (5)$$

where f is the distribution function, F_w and F_d are the wet and dry flow rates respectively at the same differential pressure, p , and D is pore diameter. The distribution function is such that the area under the plot of distribution function against pore diameter yields percentage flow through pores in the desired pore diameter range.

From the measured liquid flow rate (dry flow) liquid permeability is computed using Darcy's law. Because liquid flow rate is insensitive to pressure, $[F_w/(p_i - p_o)]$ and $[F_d/(p_i - p_o)]$ are measures of permeability.

3.The Technique

The sketch in Figure 4 illustrates the technique. Two immiscible liquids, liquid-1 and liquid-2 are selected such that liquid-2 has higher surface tension. The pores of the sample are filled with liquid-1, liquid-2 covers the sample and pressure on liquid-2 is gradually increased. The flow rate of liquid-2 through the sample is measured as a function of differential pressure from the weight gain of the liquid collection container or volume increase in a penetrometer. In order to generate the dry curve, flow rate of liquid-2 through the sample free from liquid-1 is then measured as a function of differential pressure. The results generate the dry curve.

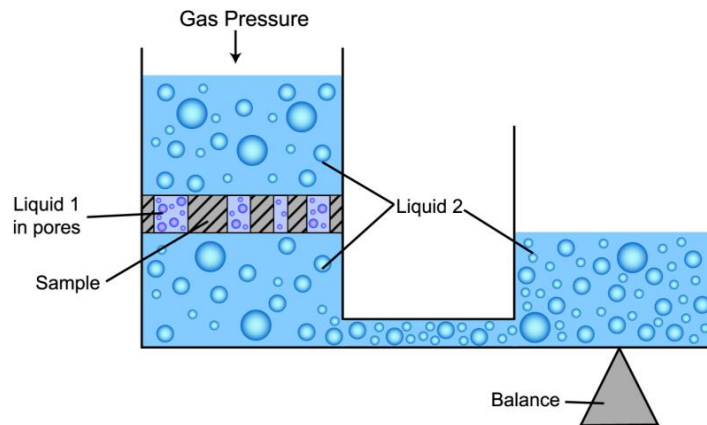


Figure 4. Principle of liquid-liquid porometry

When the flow rate is large, the liquid-liquid flow porometer is essentially a liquid permeameter. It measures the differential pressure at which the liquid flows and the flow rate of the liquid from the change of height of the liquid column in the penetrometer.

For small flow samples like membranes, the liquid-liquid flow porometer is essentially a liquid extrusion porosimeter. Figure 5 shows the liquid-liquid flow porometer. In this set up the sample is placed on a support screen in the sample chamber. The chamber below the screen is connected to a container supported on a microbalance. The chamber below the screen and the container are filled with liquid-2. The sample is wetted with wetting liquid-1. The wetted sample is placed on the screen in the sample chamber. The O-ring and the insert are then placed in the sample chamber. The wetting liquid-2 is added to the top of the sample. The sample chamber is sealed with O-rings and the piston on which pressure is pneumatically controlled through a cylinder. Gas pressure on the liquid in the sample chamber is increased. Liquid flowing out of the sample is measured as the increase in weight of the liquid in the balance. When wetting liquid-1 is out of the sample, the test is continued with decreasing pressure to obtain the dry curve. The microbalance is capable of measuring very small increases in liquid flow through the sample.

4. Application

4.1 Wetting Liquids

For tests carried out on several membranes Silwick and isopropyl alcohol were used as the wetting liquids. Surface tensions of Silwick and isopropyl alcohol are 20.1 dynes/cm and 21.7 dynes/cm respectively. In order to saturate the liquids with each other, the two liquids were vigorously mixed and held for about a day to allow separation of the saturated liquid from each other. The Silwick rich liquid was used to wet the sample. The sample was soaked in the liquid for about half an hour to completely fill all the pores. The alcohol rich phase was used to displace the Silwick rich phase from the pores and flow through the pores.

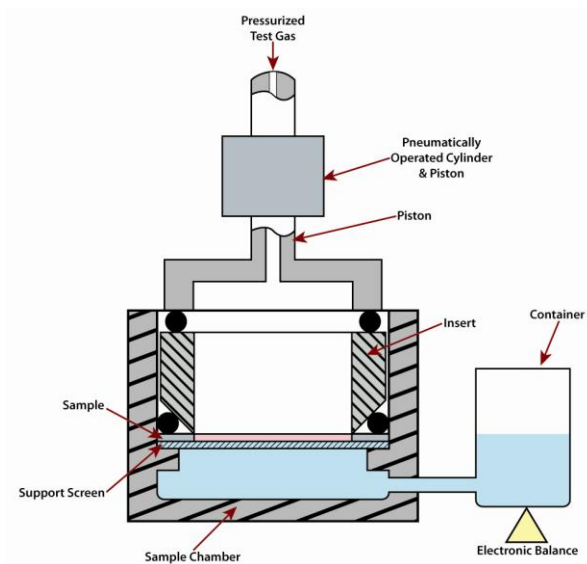


Figure 5. Liquid-Liquid Flow Porometer

4.2 Interfacial Tension between Silwick and Isopropyl Alcohol

One convenient method of finding the interfacial tension involves determine the mean flow pressure of a track etched membrane by Capillary Flow Porometry using Galwick and by Liquid-Liquid Flow Porometry using Silwick and alcohol. It follows from Equation 4 that:

$$4 \gamma_{G/A} / p_{CFP} = D_{MFPD} = 4 \gamma_{Sil./Iso.} / p_{LLP} \quad (6)$$

where $\gamma_{G/A}$ is Galwick-air interfacial tension, p_{CFP} is mean flow pressure by CFP, D_{MFPD} is mean flow pore diameter of the track etched membrane, $\gamma_{Sil./Iso.}$ is Silwick-isopropyl alcohol interfacial tension, and p_{LLP} is mean flow pressure by LLP. Equation 6 may be rewritten in the following form.

$$\gamma_{\text{Sil./Iso.}} = \gamma_{\text{G/A}} \left(\frac{\rho_{\text{LLP}}}{\rho_{\text{CFP}}} \right) \quad (7)$$

Tests on a track etched membrane yielded the following.

Mean flow pressure by CFP = 367.664 psi
 Galwick surface tension = 15.9 dynes/cm
 Mean flow pressure by LLP = 46.833 psi

Substituting in Equation 7, the Silwick-isopropyl alcohol interfacial tension became 2.021 dynes/cm.

4.3 Pore Structure of Membrane

4.3.1 Investigation using LLP

Pore Diameters: The wet and dry curves measured by LLP are shown in Figure 6. The differential pressure for initiation of flow through the wet sample, yielded bubble point pore diameter. The tortuosity factor, one was used in the computations of pore size. The bubble point pore diameter was 0.227 μm . The mean flow pressure is the differential pressure at which the wet flow is the same as half of the dry flow. The mean flow pressure is 26 psi. The mean flow pore diameter is computed from mean flow pressure. It was 0.045 μm .

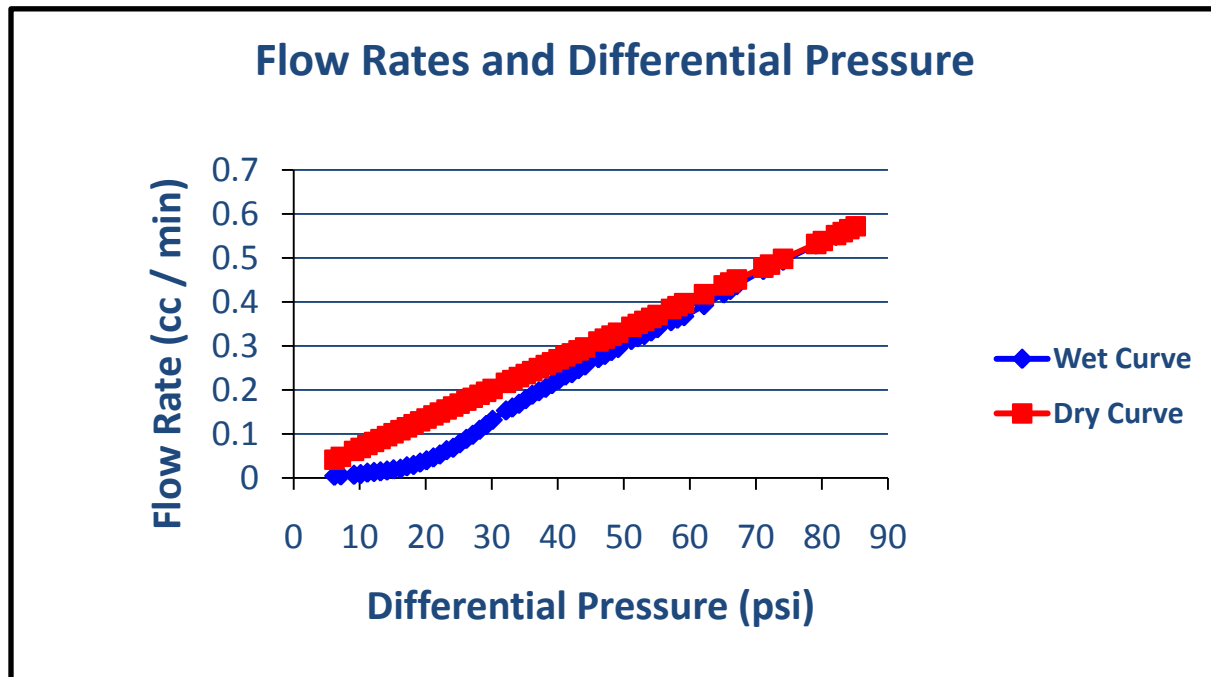


Figure 6. Wet and dry curves of membrane measured by LLP

Pore Distribution: It is given by the distribution function (Equation 5). The pore distribution presented in Figure 7 shows the distribution peak at 0.040 μm .

Liquid Permeability: The dry curve yields liquid flow rate. For example the flow rate at 80 psi differential pressure is 0.106 cc/min-cm². Liquid permeability is computed from the flow rate using Darcy's law.

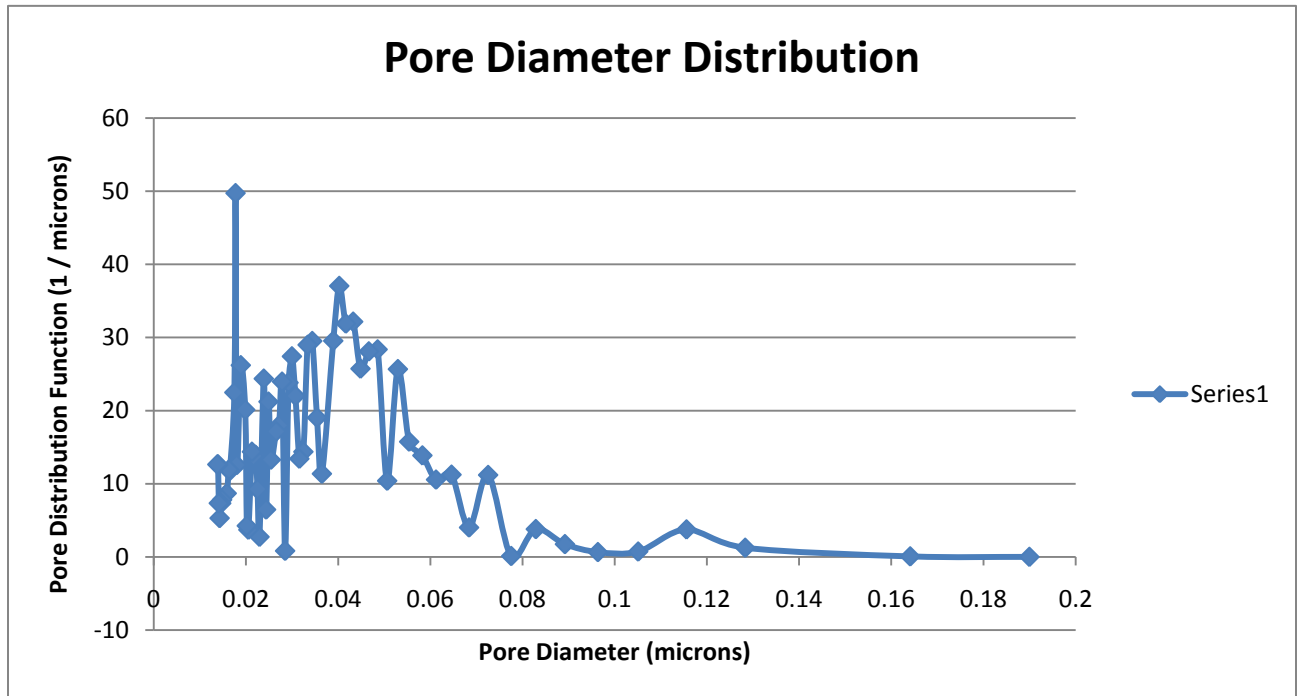


Figure 7. Pore distribution of membrane by LLP

4.3.2 Investigation Using CFP

The membrane was tested in CFP using Galwick as the testing liquid. The dry and wet curves, and the distribution function are in Figures 8 and 9 respectively. The tortuosity factor one was used in the computations of pore size. The bubble point pore diameter and the mean flow pore diameters were 0.205 μm and 0.040 μm respectively. The distribution peak is at 0.04 μm . The mean flow pressure was 202 psi. Table 1 summarizes the data. The results obtained by LLP and CFP are in good agreement with each other.

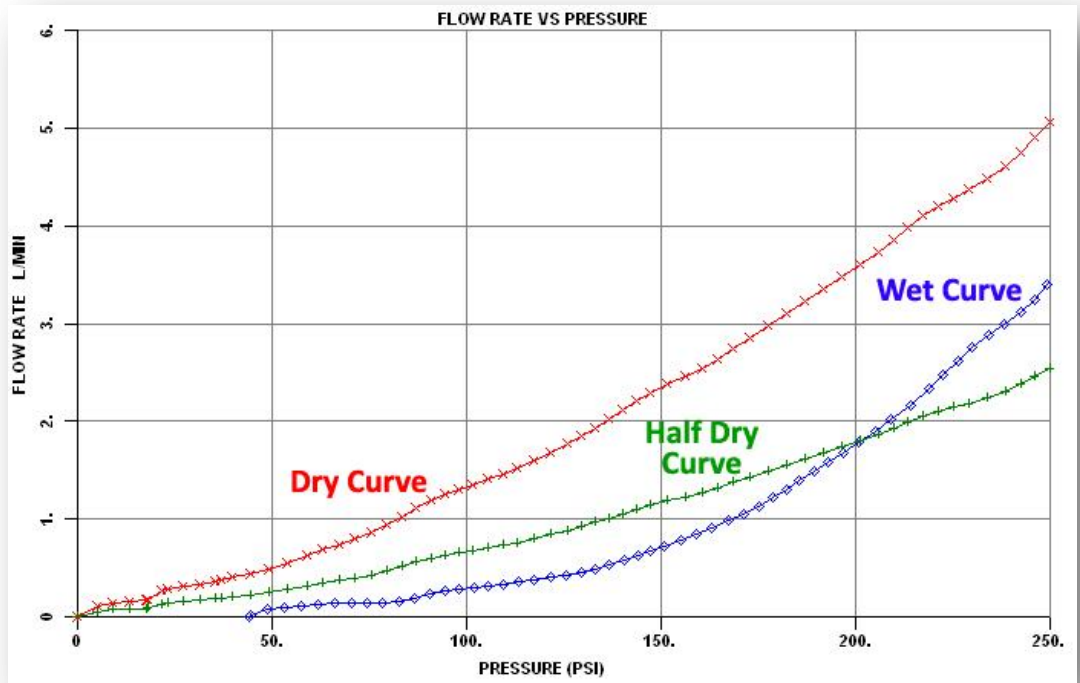


Figure 8. Dry and wet flow through of membrane measured in CFP

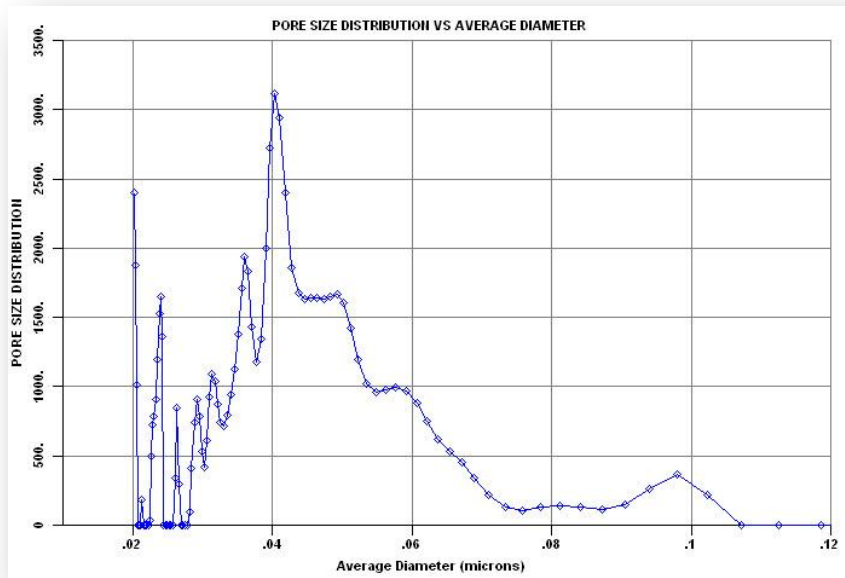


Figure 9. Pore distribution of the membrane measured by CFP

Table 1. Summary of results measurable by both techniques, LLP and CFP

| Properties of Interest | LLP | CFP |
|----------------------------------|----------|----------|
| Mean Flow Pressure, psi | 26 | 202 |
| Bubble Point, μm | 0.227 | 0.205 |
| MFPD, μm | 0.045 | 0.040 |
| Distribution Peak, μm | 0.040 | 0.040 |
| Through Pore Throat Diameters | Measured | Measured |
| Liquid Flow rate | Measured | x |
| Gas Flow Rate | x | Measured |

4.4 Pore Structure of stretched polymeric membrane

A stretched polymeric membrane was also investigated using LLP and CFP . The dry and wet curves as well as the pore distributions obtained using LLP are presented in Figures 10 and 11. The corresponding data obtained using CFP are presented in Figures 12 and 13. The results are listed in Table 2 along with the results cited above for the other membrane.

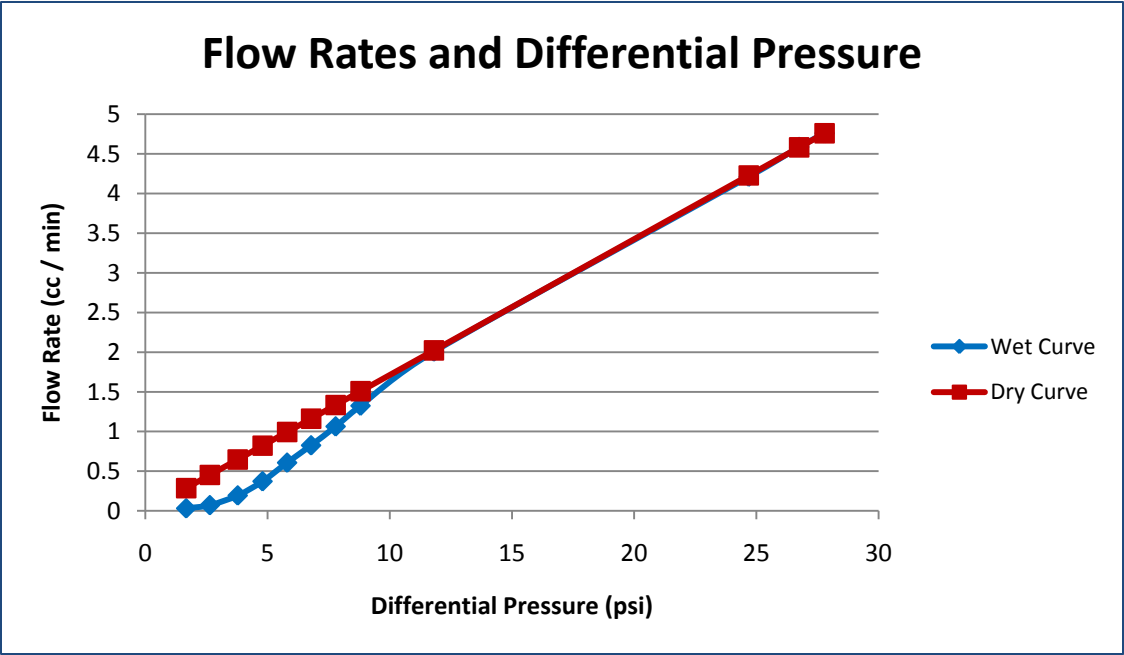


Figure 10. Dry and wet curves of stretched polymeric membrane obtained by LLP

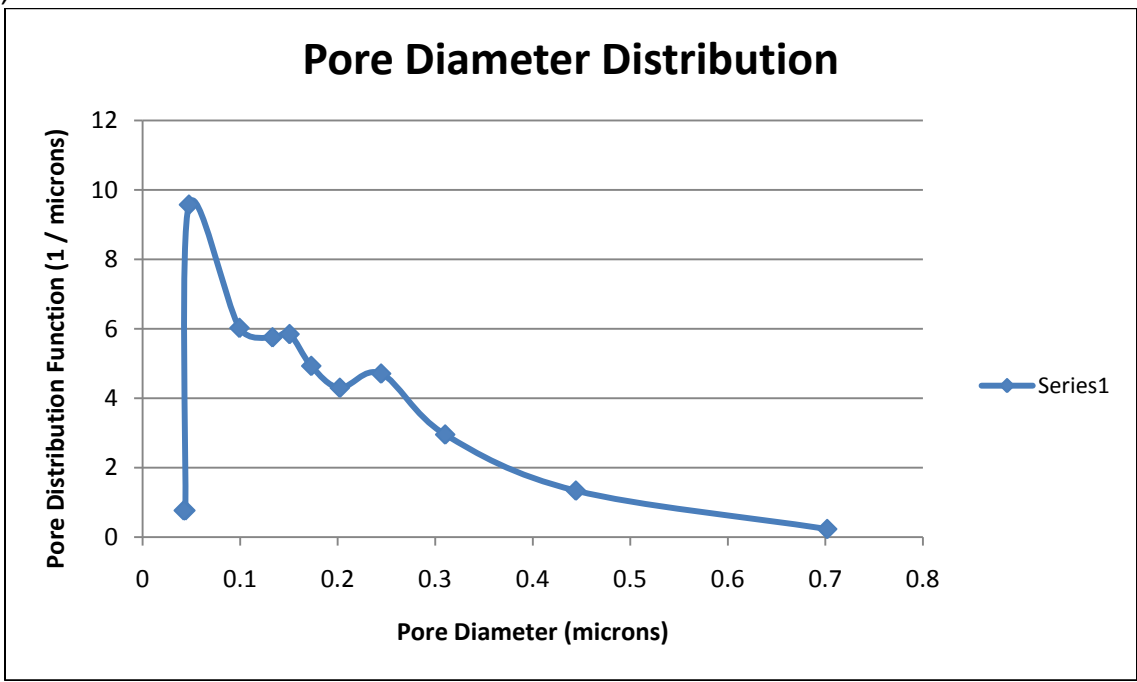


Figure 11. Pore distribution of stretched polymeric membrane obtained using LLP

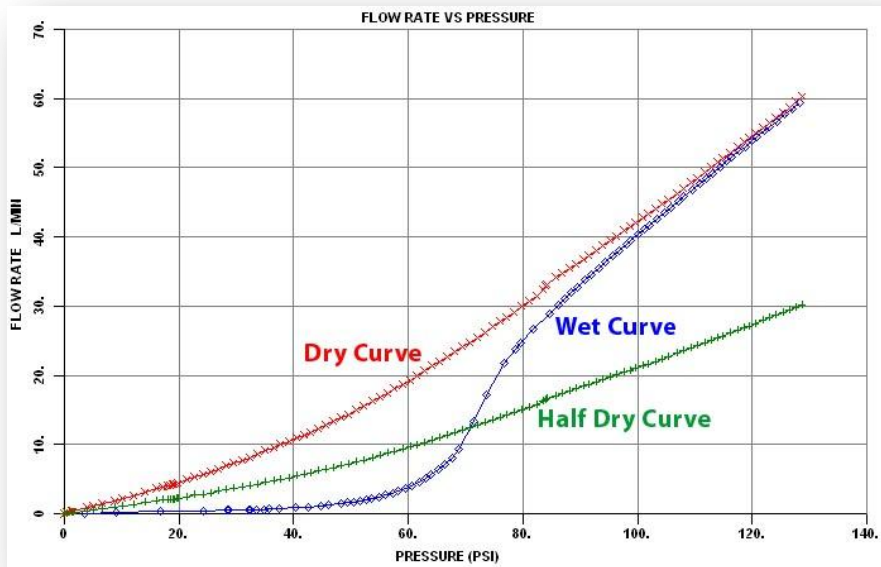


Figure 12. Dry and wet curves of stretched polymeric membrane obtained by CFP

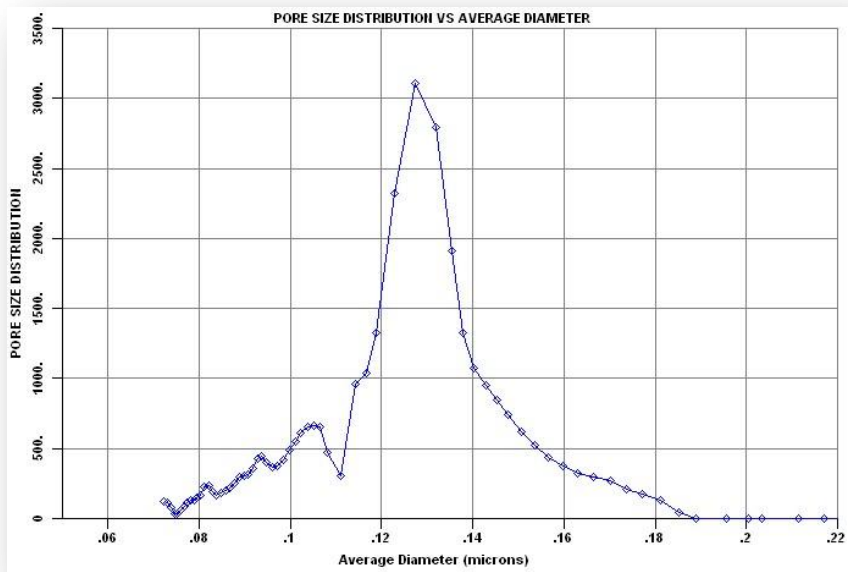


Figure 13. Pore distribution of stretched polymeric membrane obtained using CFP

Table 2. Results obtained with the two membranes using LLP and CFP

| Sample | Technique | BP, μm | MFPD, μm | Distribution | |
|-------------------|-----------|-------------------|---------------------|-----------------------|------------------|
| | | | | Peak, μm , | MF Pressure, psi |
| Membrane | CFP | 0.205 | 0.040 | 0.040 | 202 |
| | LLP | 0.227 | 0.045 | 0.040 | 26 |
| Stretched Polymer | CFP | 2.618 | 0.131 | 0.127 | 71 |
| | LLP | 1.210 | 0.223 | 0.126 | 5 |

The following characteristics of the data are of interest.

1. The test pressure required for CFP is almost an order of magnitude higher than that required for LLP. Characteristics of pressure sensitive membranes may be altered by the higher test pressures used in CFP.
2. The data suggest that the results are in good agreement.
3. MFPD measured in CFP is a little lower than that measured in LLP. This may be partly attributed to higher test pressures used in CFP.

Bubble point pore diameters are not in good agreement. This is primarily because the flow rate of the liquid at the bubble point is very small. Therefore, pressure at which the small liquid flow starts through a wet sample is not accurately detectable.

5. Strengths and Limitations of LLP and CFP

Table 3 Comparison between LLP and CFP

| Characteristics | LLP | CFP |
|---|-----------------------------------|------------------------------------|
| Test pressure | About an order of magnitude lower | About an order of magnitude higher |
| Effect of pressure On pore structure | Negligible | Can be appreciable |
| Through pore throat diameters | Measurable | Measurable |
| Smallest measurable diameter | 2 nm | 13 nm |
| Bubble point | Not accurately measurable | Accurately measurable |
| Mean Flow Pore Diameter | Measurable | Measurable |
| Pore distribution | Measurable | Measurable |
| Liquid permeability | Measurability | Not measurable |
| Gas Permeability | Not Measurable | Measurable |

6. LLP with Accurate bubble point detection capability

Liquid-Liquid Flow Porometers with attachment to measure bubble point accurately are available. The technique used in CFP for accurate bubble point measurement is incorporated the Liquid-Liquid Flow Porometer. Because bubble points are the largest pore diameters, the required test pressures are normally not high.

7. Summary and Conclusion

The Liquid-Liquid Flow Porometry is a novel technique which is capable of measuring through pore throat diameters, mean flow pore diameters, and pore distribution, accurately using test pressures that are an order of magnitude less than those used in Capillary Flow Porometry. LLP cannot measure bubble point accurately, but suitable attachments can overcome this problem. LLP has the added advantage of measuring liquid permeability which is measurable in CFP only with suitable attachments.

8. References

1. Akshaya Jena and Krishna Gupta, 'Characterization of Pore Structure of Filtration Media', Fluid/Particle Separation Journal, Vol. 14, No. 3, 2002, pp. 227-241.
2. Akshaya Jena and Krishna Gupta, 'Advances in pore structure evaluation by porometry', Chemical Engineering and Technology, Vol. 33, No. 8, 2010, pp.1241-1250.